

A laser ultrasound transducer using carbon nanofibers–polydimethylsiloxane composite thin film

Bao-Yu Hsieh, Jinwook Kim, Jiadeng Zhu, Sib0 Li, Xiangwu Zhang, and Xiaoning Jiang

Citation: [Applied Physics Letters](#) **106**, 021902 (2015); doi: 10.1063/1.4905659

View online: <http://dx.doi.org/10.1063/1.4905659>

View Table of Contents: <http://scitation.aip.org/content/aip/journal/apl/106/2?ver=pdfcov>

Published by the [AIP Publishing](#)

Articles you may be interested in

[Thermal conductivity of high performance carbon nanotube yarn-like fibers](#)

J. Appl. Phys. **115**, 174306 (2014); 10.1063/1.4874737

[Carbon nanotube composite optoacoustic transmitters for strong and high frequency ultrasound generation](#)

Appl. Phys. Lett. **97**, 234104 (2010); 10.1063/1.3522833

[Photoacoustic technique to measure beam profile of pulsed laser systems](#)

Rev. Sci. Instrum. **80**, 054901 (2009); 10.1063/1.3125625

[Direct imaging of current paths in multiwalled carbon nanofiber polymer nanocomposites using conducting-tip atomic force microscopy](#)

J. Appl. Phys. **104**, 083708 (2008); 10.1063/1.3000458

[Numerical analysis of acoustic wave propagation in layered carbon nanofiber reinforced polymer composites](#)

J. Appl. Phys. **104**, 043522 (2008); 10.1063/1.2973039

An advertisement for Keysight B2980A Series Picoammeters/Electrometers. The ad features a red and white color scheme. On the left, text reads 'Confidently measure down to 0.01 fA and up to 10 PΩ' and 'Keysight B2980A Series Picoammeters/Electrometers'. Below this is a red button with the text 'View video demo'. On the right, there is an image of the Keysight B2980A device and the Keysight Technologies logo.

A laser ultrasound transducer using carbon nanofibers–polydimethylsiloxane composite thin film

Bao-Yu Hsieh,¹ Jinwook Kim,¹ Jiadeng Zhu,² Sibol Li,¹ Xiangwu Zhang,² and Xiaoning Jiang^{1,a)}

¹Department of Mechanical and Aerospace Engineering, North Carolina State University, Raleigh, North Carolina 27695, USA

²Fiber and Polymer Science Program, Department of Textile Engineering, Chemistry and Science, North Carolina State University, Raleigh, North Carolina 27695, USA

(Received 2 September 2014; accepted 27 December 2014; published online 12 January 2015)

The photoacoustic effect has been broadly applied to generate high frequency and broadband acoustic waves using lasers. However, the efficient conversion from laser energy to acoustic power is required to generate acoustic waves with high intensity acoustic pressure (>10 MPa). In this study, we demonstrated laser generated high intensity acoustic waves using carbon nanofibers–polydimethylsiloxane (CNFs-PDMS) thin films. The average diameter of the CNFs is 132.7 ± 11.2 nm. The thickness of the CNFs film and the CNFs-PDMS composite film is 24.4 ± 1.43 μ m and 57.9 ± 2.80 μ m, respectively. The maximum acoustic pressure is 12.15 ± 1.35 MPa using a 4.2 mJ, 532 nm Nd:YAG pulsed laser. The maximum acoustic pressure using the CNFs-PDMS composite was found to be 7.6-fold (17.62 dB) higher than using carbon black PDMS films. Furthermore, the calculated optoacoustic energy conversion efficiency K of the prepared CNFs-PDMS composite thin films is 15.6×10^{-3} Pa/(W/m²), which is significantly higher than carbon black-PDMS thin films and other reported carbon nanomaterials, carbon nanostructures, and metal thin films. The demonstrated laser generated high intensity ultrasound source can be useful in ultrasound imaging and therapy. © 2015 AIP Publishing LLC.

[<http://dx.doi.org/10.1063/1.4905659>]

High power ultrasound transducers can be used to apply acoustic wave-induced thermal energy, radiation force, and cavitation effects on tissues for therapy benefits. At present, piezoelectric transducers are dominantly adopted for ultrasound diagnosis and therapy. Piezoelectric high intensity focused ultrasound (HIFU) transducers for therapy usually feature large apertures (several centimeters), large focusing volumes (1–3 mm in lateral direction and around 1 cm in axial direction), high driving voltage, and relatively low frequencies (1–5 MHz),¹ which eliminates some applications on therapies. High frequency HIFU with spatial and temporal confinement could be used for precision therapies.² However, due to the fact that the tissue attenuation increases with frequency, higher acoustic intensity is required for high frequency HIFU to reach the similar treating effect as using the conventional HIFU. To match this acoustic intensity criterion, a large aperture ultrasound transducer may be adopted and driven with a high voltage. Even so, it is still challenging to achieve the required therapeutic pressure in the high frequency regime by using piezoelectric HIFU transducers due to the mismatched impedance for a large aperture and the de-poling problem with high driving voltages.³ Moreover, the bulky piezoelectric HIFU transducers and the associated high driving voltage render them inappropriate for interventional therapy⁴ and imaging⁵ applications. As an alternative method, laser-generated ultrasound, which has the capability of generating high frequency and wideband acoustic waves, can be used to address the aforementioned challenges of

conventional HIFU transducers.⁶ The most common mechanism of laser-generated ultrasound is based on the thermoelastic effect, which is also called the photoacoustic or optoacoustic effect.⁷ In a laser ultrasound transducer, the material absorbs pulsed laser energy, leading to a transient thermal expansion, generating an ultrasonic wave propagating out from the absorber. The sketch of a laser generated ultrasound transducer is shown in Fig. 1. The laser light can shine on flat or concave absorbing film to generate un-focused or focused ultrasound, respectively. In this scheme, the laser spot defines the active element of ultrasound generation, and the element size can be manipulated with conventional optics from several microns to centimeters. This approach provides a strategy to miniaturize the ultrasound probe and even the high density array with multiple beams. One example is a laser ultrasound transducer using optical fibers, which was demonstrated by coating high optical absorption materials on the site of optical output from the optical fibers.^{8–10} The size of this handheld probe can be minimized to several hundreds of microns, and such a small probe can be integrated into interventional medical devices. In addition, no electromagnetic interference is expected, as there are no electronic components in the laser ultrasound transducers. The laser ultrasound transducers can be integrated with piezoelectric transducers or optical based ultrasound sensors to form all-optical ultrasound transducers for a broad range of biomedical applications.^{11–14}

In the laser ultrasound transducers, the optical absorbing thin film with high optical absorption and high thermal expansion is a critical component. Many different absorbing

^{a)}Electronic mail: xjiang5@ncsu.edu

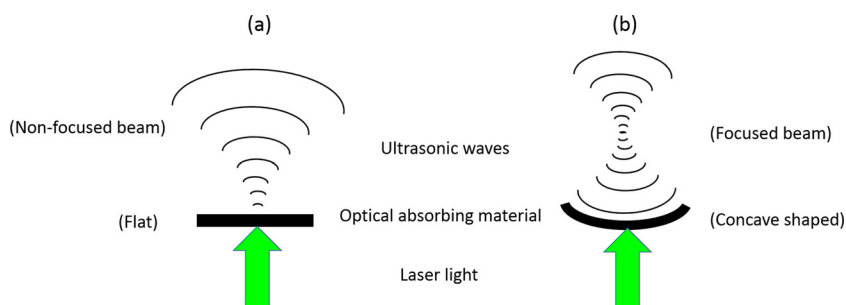


FIG. 1. Sketch of (a) non-focused and (b) focused laser generated ultrasound transducer.

thin films have been studied. The metallic films (Mo,¹⁵ Al,¹⁵ and Cr¹⁶) were used to generate high frequency ultrasound (>50 MHz), but the conversion efficiency (i.e., $K_{Cr} \sim 10^{-5}$, K : optoacoustic conversion efficiency)⁶ from optical to thermoelastic power is poor due to the low thermal expansion coefficient of the metallic films. Polydimethylsiloxane (PDMS) has been used in fabrication of an elastomeric film to overcome this limitation based on its high thermal coefficient of volume expansion of $\alpha = 310 \times 10^{-6} \mu\text{m}/\mu\text{m}/^\circ\text{C}$. The PDMS was mixed with the carbon black powders with high optical absorption and then spin coated onto the transparent glass substrate. The conversion efficiency was improved by over 20 dB compared with that of the Cr films.¹⁶ A two-dimensional gold nanoparticle (AuNP) array with an overlying PDMS layer was adopted to improve the laser ultrasound amplitude (~ 5 dB) at the frequency range over 50 MHz compared to those using carbon black-PDMS thin films.¹⁷ The carbon-based nanomaterials, including the graphene¹⁸ and the carbon nanotube (CNT) composite,¹⁹ were also considered as the optical absorbing films for laser ultrasound transducers. The reduced graphene oxide coated aluminum film showed the capability of generating acoustic pressure of 7.5 MPa near the transducer surface, which is approximately 64 fold stronger than those using the aluminum thin film alone.¹⁸ For the CNT-PDMS composite, the amplitude of generated ultrasound signals can be 18 fold stronger than that of the Cr film and 5 fold stronger than that of the AuNP-PDMS film.¹⁹ However, the maximum acoustic pressure from these previous works are not over 10 MPa with a planar thin film design. The pressure amplitude was further enhanced by coating the CNT-composite on the concave lens with a focusing gain. Baac *et al.* demonstrated an approach to generate high frequency (>15 MHz) and high acoustic pressure (>50 MPa) focused ultrasound using a concave shaped CNT film,⁶ which is the highest reported laser-generated acoustic pressure so far. This high frequency and unprecedented acoustic pressure suggest a high precision ultrasound therapeutic tool for micro-scale ultrasonic fragmentation of solid materials, leading to single-cell surgery in terms of removing the cell from the substrate.⁶ Albeit the initial success on laser ultrasound using various thin film absorbers, continuous enhancement of optoacoustic conversion efficiency is needed to advance the laser ultrasound transducer technology. In this paper, we investigated a carbon nanofibers-PDMS (CNFs-PDMS) composite thin film for laser ultrasound. More specifically, we designed a CNFs-PDMS thin film consisting of a layer of CNFs film sandwiched between a transparent glass substrate and a PDMS layer. A 532 nm Nd:YAG pulsed laser was used for

delivering the laser energy to the film. The laser-generated acoustic wave from this CNFs-PDMS composite film was characterized and compared with that from carbon black PDMS films.

Among carbon nanomaterials and nanostructures, the CNFs are cylindrical nanostructures with graphene layers showing strong light absorption and high thermal conductivity (~ 1950 W/m K),²⁰ which may result in a highly efficient energy transfer from laser light to thermal energy. Since carbon-based nanostructures provide a huge interfacial area to transfer heat quickly to the surrounding medium, the CNFs film may be a good candidate to act as a transformer for laser generated ultrasound. In addition, CNFs are cost-effective materials compared with CNTs and can be easily fabricated and handled in the experiment. To date, the CNFs have not been demonstrated in high intensity laser generated ultrasound.

For the CNFs thin film preparation, an amount of 2.4 g Polyacrylonitrile (PAN, Mw = 150 000, Sigma-Aldrich, St. Louis, MO) was added to 30 g *N,N*-Dimethylformamide (DMF). The mixture was first stirred at 50 °C for 24 h to produce a viscous and homogeneous solution, which was then transferred into a plastic syringe with a tip needle. The needle-aluminum collector distance of 15 cm and the feed rate of 0.75 ml/min were set in the syringe pump system (NE-1000, New Era Pump Systems Inc., Farmingdale, NY). A high voltage of 15 kV from the high voltage power supply (ES40P-20 W/DAM, Gamma High Voltage Research, Ormond Beach, FL) was applied for the electrospinning of the obtained solution. The as-spun fibers were first stabilized at 250 °C for 2 h in air with a heating rate of 5 °C/min, and then carbonized under a nitrogen atmosphere at 900 °C for 2 h with a heating rate of 2 °C/min. After carbonization, the CNFs were a paper-like thin film. The scanning electron microscopy (SEM) photograph of the fabricated CNFs thin film is shown in Fig. 2(a). The average diameter of the CNFs was 132.7 ± 11.2 nm, and the thickness of the CNFs thin film was 24.4 ± 1.43 μm . The

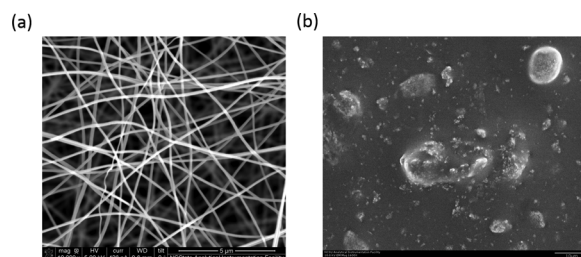


FIG. 2. SEM photograph of (a) CNFs thin film (10000 \times) and (b) carbon black thin film (1600 \times).

fabricated CNFs paper-like thin film was then attached to a 1 mm thick flat glass substrate (Plain glass micro slides, Thermo Fisher Scientific, Pittsburgh, PA), and then the pure PDMS was spun at 3000 rpm and coated on the top of the CNFs film and cured at 65 °C for 1 h. The sandwich structure is schematically shown in Fig. 3. The total thickness of the CNFs-PDMS composite was $57.9 \pm 2.80 \mu\text{m}$. The UV-VIS-NIR spectrometer (Agilent Cary 5000 UV-VIS-NIR, Santa Clara, CA) was utilized to measure the optical density (OD), optical transmission, and reflection of the film at the wavelength of 532 nm. The optical transmission and the reflection of the CNFs-PDMS film were 0.001% and 4.13%, respectively. Thus, the corresponding OD for the CNFs-PDMS film is 5. The optical absorption measured at different spots on the $2 \text{ cm} \times 2.5 \text{ cm}$ CNFs-PDMS film was $95 \pm 0.72\%$, equally distributed across the film surface, so the optical absorption across the film surface is macroscopically homogeneous. For comparison, the standard carbon black PDMS thin film consisting of the carbon black powders mixed with the PDMS solution was also prepared. The conversion efficiency of the photoacoustic effect is linearly proportional to the optical absorption coefficient of materials, which is corresponding to the concentration of absorbers (the carbon black). The concentration of carbon black was 61.28% (% w/w), which is the maximum concentration we can apply since the film cannot be cured well when the carbon black is over this amount. The mixture was spun at 3000 rpm and coated on the glass substrate and cured at 65 °C for 1 h. The thickness of the carbon black PDMS film was $30 \mu\text{m}$, measured by the thickness gauge (MS 45, Heidenhain Corp., Schaumburg, IL). The thickness is close to what has been reported ($25 \mu\text{m}$).¹⁶ The thickness of the carbon black PDMS film cannot be further reduced because the addition of the carbon black significantly increases the viscosity of the mixture with this concentration. The SEM photograph of the carbon black thin film is shown in Fig. 2(b). In this image, the particle size is in the range of 1–10 μm .

The experimental setup for the laser ultrasound generation and characterization is shown in Fig. 4. The excitation laser source was the 532 nm Q-switched Nd:YAG pulsed laser (Minilite I, Continuum Inc., Santa Clara, CA) with a pulse duration of 4 ns and a pulse repetition frequency of 10 Hz. The beam diameter was 12 mm after passing through a 4 \times beam expander (HB-4 \times , Newport Optics Inc., Irvine, CA). The laser beam penetrated through the glass optical window on the water tank and shined on the CNFs-PDMS or the carbon black-PDMS thin films. The CNFs or the carbon black thin film absorbed laser energy, generating heat that was then transferred to the high thermal expansion material, PDMS, and resulted in acoustic wave generation. The spatial

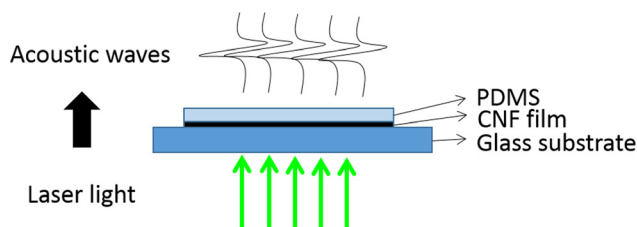


FIG. 3. Structural sketch of the CNFs-PDMS thin film.

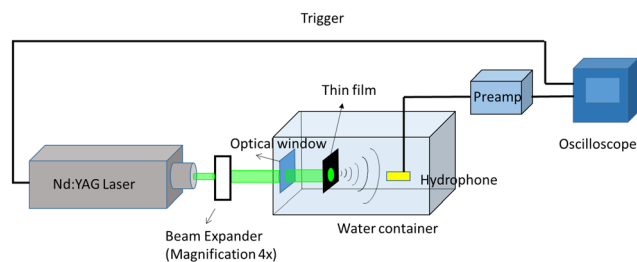


FIG. 4. Experimental setup for laser ultrasound generation and characterization.

beam profile of the laser beam is a Gaussian distribution, with the acoustic pressure at the center much higher than that on the off-axis location. A high-frequency hydrophone (HGL-0085, ONDA Corp., Sunnyvale, CA) was utilized to detect the generated ultrasound signals. The signals were amplified by a preamplifier and then recorded by an oscilloscope (DSO7104B, Agilent, CA). The external trigger from the laser system was utilized to synchronize the time series of laser excitation with the oscilloscope data acquisition.

During the acoustic characterization, the hydrophone was initially mounted close to the thin film to collect the signals with maximum acoustic pressure. To measure the acoustic attenuation with distance, the hydrophone was attached on a precision stage and received the signals at different distances along the wave propagation axis from 0.78 mm to 41.48 mm. At each position, 4 measurements were conducted, and the average peak-to-peak value was then calculated.

The acoustic signals were received by the hydrophone at a position of 3.65 mm away from the absorbing thin film surface to calculate the acoustic pressure. The acoustic pressure waveforms of laser-generated ultrasound using the CNFs-PDMS and the carbon black PDMS thin films under the same laser fluence ($3.71 \text{ mJ}/\text{cm}^2$) are shown in Fig. 5(a). The peak pressure generated from the CNFs-PDMS film was $12.15 \pm 1.35 \text{ MPa}$, which is 7.6 fold (17.62 dB) stronger than that from the carbon black PDMS film. The frequency spectra of the two generated signals are shown in Fig. 5(b). Both spectra were normalized to the maximum amplitude of the CNFs-PDMS signal. The -6 dB bandwidth of these two signals was 7.63 and 7.84 MHz, respectively. The frequency distributions and bandwidth between these two films were close to each other because of the similar optical penetration depth in these two carbon absorbers,²¹ although the amplitude generated from CNT-PDMS films was $\sim 17.6 \text{ dB}$ higher than that of carbon black film.

Fig. 6 shows the acoustic amplitude at different axial distances. The ultrasonic decay in this test is primarily due to the relaxation of higher frequency components of shock waves. Since the shock wave front contains more high frequency components, they are attenuated faster than other parts of the shock wave profile. After traveling a few centimeters in water, the amplitude of the shock wave reduces and its rise time increases, which means high frequency parts are attenuated in the short distances. In addition, this “shock effect” may also explain the faster decay of the CNFs sample, since the higher amplitude pressure probably leads to a much stronger shock (Fig. 6). The decay trends are consistent with the numerical and experimental results.^{18,22} In Fig. 6, it was found that the acoustic pressure from the CNFs-PDMS film is

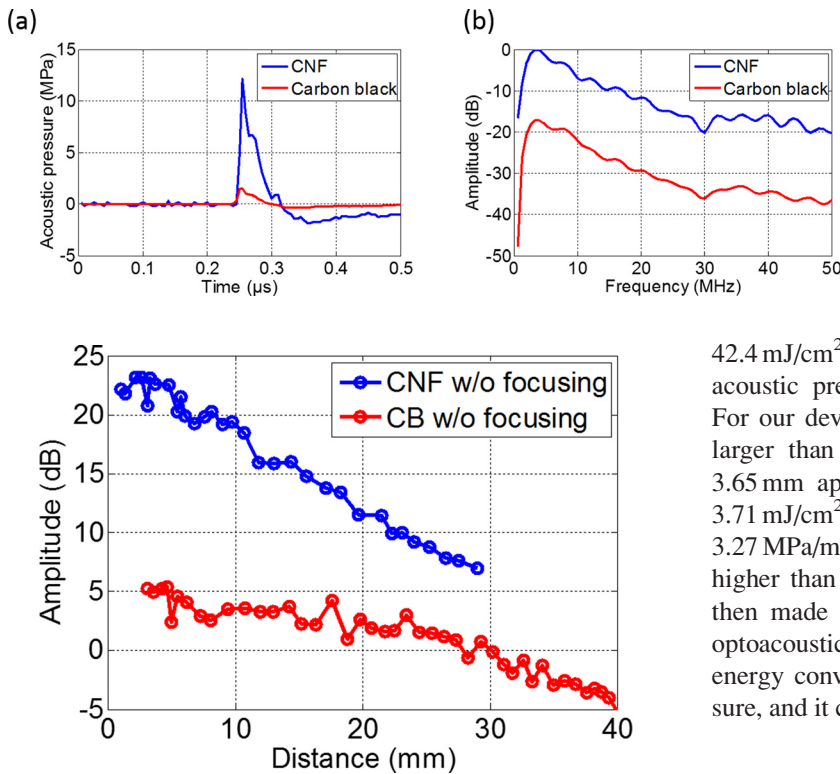


FIG. 6. The peak-to-peak acoustic amplitude along the axial direction.

much higher than that of the carbon black film at all different axial distances. The pressure fluctuations are due to the fluctuations of the excitation laser energy although 4 measurements for averaging were conducted at the same location to minimize the effect by the laser fluctuations. The stability of the laser energy we measured is $\pm 9.17\%$, which may cause the fluctuations of measured acoustic pressures.

The measured acoustic pressure of the prototyped laser ultrasound transducers was compared with the published results (Table I). The maximum acoustic pressure generated from the CNFs-PDMS was 12.15 MPa with 4.2 mJ (3.71 mJ/cm^2) laser energy. The 4.2 mJ is the highest laser energy of the laser used in this study. The obtained acoustic pressure is the highest value compared with that generated from other planar thin films.^{8,10,17,18} However, the value is lower than that of generated by the concave shaped CNT composite.⁶ The higher acoustic pressure reported in Ref. 6 was attributed to the much higher laser energy ($>50 \text{ mJ/pulse}$) and with focusing gain of 54 by the concave optoacoustic lens. In the Baac's device, the peak positive pressure was 22 MPa with the focusing gain of 54. It means that the pressure on the surface was about 0.41 MPa. The laser fluence for this case was

42.4 mJ/cm^2 . Thus, the energy conversion coefficient (surface acoustic pressure/laser fluence)¹⁰ was $0.0097 \text{ MPa/mJ/cm}^2$. For our device, the peak pressure on the surface should be larger than 12.15 MPa which was the measured value at 3.65 mm apart from the source and the laser fluence was 3.71 mJ/cm^2 . Thus, the energy conversion coefficient was 3.27 MPa/mJ/cm^2 , which is more than two orders (337 fold) higher than Baac's CNT device. A further comparison was then made on the optoacoustic conversion efficiency. The optoacoustic conversion efficiency (K) is defined by the energy conversion from the laser light to the acoustic pressure, and it can be expressed as⁶

$$K = \frac{\left| \frac{1}{T} \int_T P(t) dt \right|}{\frac{1}{T} \int_T I(t) dt} \quad [Pa/(W/m^2)], \quad (1)$$

where $P(t)$ is the average acoustic pressure and $I(t)$ is the average optical intensity during the period T ($=100 \text{ ms}$). In Ref. 6, the K value of the CNTs optoacoustic lens with the focusing gain of 54 is $1.4 \times 10^{-3} \text{ Pa/(W/m}^2)$, so the K value on the lens surface can be estimated to be $2.59 \times 10^{-5} \text{ Pa/(W/m}^2)$. The K value of the CNFs-PDMS thin films is $1.56 \times 10^{-2} \text{ Pa/(W/m}^2)$, which is also two orders (602 fold) higher than that of the Baac's CNT material. These initial results suggest that CNFs-PDMS composite films can serve as a promising transducer for laser ultrasound.

In this study, we investigated CNFs-PDMS composite thin films for laser ultrasound transducers. The average diameter of the CNFs prepared for the study was $132.7 \pm 11.2 \text{ nm}$ and the total thickness of the CNFs-PDMS composite film was $57.9 \pm 2.80 \mu\text{m}$. The maximum peak-to-peak pressure was 12.15 MPa, which is 7.6 fold (17.62 dB) stronger than that of the carbon black PDMS film under the excitation of the same laser energy of 4.2 mJ (532 nm Nd:YAG laser). The acoustic pressure generated in this study is the highest value among all the published pressure values using planar thin

TABLE I. Acoustic pressure and experimental parameters comparison.

Material	Peak pressure	Laser energy	Aperture	Energy density	Shape
CNTs-PDMS film ⁶	22 MPa	N/A	6 mm	42.4 mJ/cm^2	Focused
Periodic gold nanopores ⁸	2.73 kPa at 1.5 mm	$3 \mu\text{J}$	$125 \mu\text{m}$	24.45 mJ/cm^2	Optical fiber
Multiwall CNTs/PDMS mixture ¹⁰	4.5 MPa	$11.4 \mu\text{J}$	$200 \mu\text{m}$	36.3 mJ/cm^2	Optical fiber
2D gold nanostructure ¹⁷	1.5 MPa	100 nJ	$25 \mu\text{m}$	20.37 mJ/cm^2	Planar
Reduced graphene oxide coated thin aluminum film ¹⁸	7.5 MPa	N/A	N/A	43.28 mJ/cm^2	Planar
Carbon black/PDMS mixture	2.13 MPa	4.2 mJ	12 mm	3.71 mJ/cm^2	Planar
CNFs-PDMS film	12.15 MPa	4.2 mJ	12 mm	3.71 mJ/cm^2	Planar

films. Furthermore, the calculated optoacoustic energy conversion efficiency K of the prepared CNFs-PDMS thin films is $15.6 \times 10^{-3} \text{ Pa}/(\text{W}/\text{m}^2)$, which is significantly higher than that of the carbon black-PDMS thin films and other reported carbon nanomaterials, carbon nanostructures, and metal thin films. This finding strongly suggests that CNFs-PDMS thin film is the promising composite for efficient laser ultrasound transducers for a broad range of ultrasound applications.

The authors would like to thank Dr. Nancy Allbritton and Dr. Angela Proctor of University of North Carolina at Chapel Hill for their help in the use of Nd:YAG laser system for the experiments. BH and XJ would also like to acknowledge the financial support from NIH under the grant 1R01EB015508.

¹Y.-F. Zhou, *World J. Clin. Oncol.* **2**, 8 (2011).

²G. T. Haar and C. Coussios, *Int. J. Hyperthermia* **23**, 89 (2007).

³R. Liu, H. H. Kim, J. M. Cannata, G.-S. Chen, and K. K. Shung, in *IEEE Ultrasonics Symposium* (IEEE, 2007), p. 949.

⁴Y. Okumura, M. W. Kolasa, S. B. Johnson, T. J. Bunch, B. D. Henz, C. J. O'Brien, D. V. Miller, and D. L. Packer, *J. Cardiovasc. Electrophysiol.* **19**, 945 (2008).

⁵S. E. Nissen and P. Yock, *Circulation* **103**, 604 (2001).

⁶H. W. Baac, J. G. Ok, A. Maxwell, K.-T. Lee, Y.-C. Chen, A. J. Hart, Z. Xu, E. Yoon, and L. J. Guo, *Sci. Rep.* **2**, 989 (2012).

⁷R. M. White, *J. Appl. Phys.* **34**, 3559 (1963).

⁸Y. Tian, X. Zou, H. Felemban, C. Cao, and X. Wang, *Opt. Eng.* **52**, 065005 (2013).

⁹J. Tian, Q. Zhang, and M. Han, *Opt. Express* **21**, 6109 (2013).

¹⁰R. J. Colchester, C. A. Mosse, D. S. Bhachu, J. C. Bear, C. J. Carmalt, I. P. Parkin, B. E. Treeby, I. Papanikolaou, and A. E. Desjardins, *Appl. Phys. Lett.* **104**, 173502 (2014).

¹¹Y. Hou, J.-S. Kim, S. Ashkenazi, M. O'Donnell, and L. J. Guo, *Appl. Phys. Lett.* **91**, 073507 (2007).

¹²B.-Y. Hsieh, S.-L. Chen, T. Ling, L. J. Guo, and P.-C. Li, *Opt. Express* **20**, 1588 (2012).

¹³R. Nuster, N. Schmitner, G. Wurzinger, S. Gratt, W. Salvenmoser, D. Meyer, and G. Paltauf, *J. Biophotonics* **6**, 549 (2013).

¹⁴B.-Y. Hsieh, S.-L. Chen, T. Ling, L. J. Guo, and P.-C. Li, *Photoacoustics* **2**, 39 (2014).

¹⁵R. J. von Gutfeld and H. F. Budd, *Appl. Phys. Lett.* **34**, 617 (1979).

¹⁶T. Buma, M. Spisar, and M. O'Donnell, *Appl. Phys. Lett.* **79**, 548 (2001).

¹⁷Y. Hou, J.-S. Kim, S. Ashkenazi, M. O'Donnell, and L. J. Guo, *Appl. Phys. Lett.* **89**, 093901 (2006).

¹⁸S. H. Lee, M. Park, J. J. Yoh, H. Song, E. Y. Jang, Y. H. Kim, S. Kang, and Y. S. Yoon, *Appl. Phys. Lett.* **101**, 241909 (2012).

¹⁹H. W. Baac, J. G. Ok, H. J. Park, T. Ling, S.-L. Chen, A. J. Hart, and L. J. Guo, *Appl. Phys. Lett.* **97**, 234104 (2010).

²⁰J. Heremans, I. Rahim, and M. S. Dresselhaus, *Phys. Rev. B* **32**, 6742 (1985).

²¹E. Biagi, F. Margheri, and D. Menichelli, *IEEE Trans. Ultrason. Ferroelectr. Freq. Control* **48**, 1669 (2001).

²²W. Chen, O. Maurel, C. La Borderie, T. Reess, A. De Ferron, M. Matallah, G. Pijaudier-Cabot, A. Jacques, and F. Rey-Bethbeder, *J. Heat Mass Transfer* **50**, 673 (2014).